DOI: 10.1002/ejic.201001360

Single-Step Synthesis of Ruthenium Catalytic Nanocrystallites in a Stable Carbon Support

Jose M. Calderon-Moreno,*[a] Vilas G. Pol,[b] and Monica Popa[c]

Keywords: Ruthenium / Carbon / Nanoparticles / Electron microscopy / Green chemistry

Metallic Ru nanoparticles have been prepared and incorporated in a protective carbon support by the decomposition of a single organometallic precursor, Ru^{III} acetylacetonate, under autogenic conditions in a single-step process in the absence of any solvents or stabilizers. The product structure was confirmed by X-ray diffraction, Raman spectroscopy, scanning electron microscopy, energy dispersive spectroscopy, scanning transmission electron microscopy, transmission electron microscopy and high resolution transmission electron microscopy. Measurements demonstrated the exclusive presence of hexagonal metallic ruthenium nanoparticles with a homogeneous size of 2–4 nm in a carbon supporting matrix, forming a high loading Ru catalyst with a muffin cookie like structure. The mechanism of the process is explained by the nucleation of Ru crystalline nuclei before carbon deposits on the Ru nanocrystallites, in an early stage of nanoparticle growth, during the single precursor decomposition. The carbon acts as a protective support, preventing further Ru nanoparticle growth, agglomeration or sintering. The catalytic properties have been tested by the hydrogenation of benzene to cyclohexane, and show high activity, full conversion of benzene, 100 % selectivity for cyclohexane and good recyclability.

Introduction

Nanosized particles of Pt group metals exhibit peculiar properties making them excellent catalysts for many chemical reactions, but their catalytic activity is strongly dependent on the mean particle size, shape, particle-size distribution and composition.[1–5] Their use as advanced and modern materials in high technology (electronics, optics, catalysis), because of the quantum size effect,[6] requires uniform, non-agglomerated particles with controlled mean size and a narrow size distribution. An effective control of particle size continues to be the most challenging task for the research involving the synthesis of colloidal metal dispersions.[7,8] A synthetic method that enables good control over these parameters is needed, as the difficulty of developing a low-cost, low-waste and reproducible synthesis route on a large scale is still to be encountered.[9,10]

As an important member of the group of platinum metals, Ru nanoparticles have been known to show unique activities as catalysts;[11,12] small Ru particles can be used as quantum dots for understanding the quantum size effect and for the design of new optic and electronic materials.[13] Ru nanocatalysts are attractive for catalytic processes of great industrial interest such as ammonia synthesis[12] or hydrogenation of phenol.[9] The preparation of Ru nanoparticles is a real challenge since it is less investigated[9] as compared with Pt[14–16] or Pd nanoparticles,[16,17] presumably because of the difficulties associated with ruthenium reduction as compared with the other precious metals.

Methods reported for the synthesis of Ru nanoparticles are based on chemical[18–21] and electrochemical reduction,[22] decomposition of organometallic precursors,[23,24] sonochemical decomposition,[25–27] UV photolysis[28] and metal vapour deposition.[29] Among these methods, reduction by chemical agents has been the most extensively studied: the use of polyol as a reducing agent is particularly approached by different groups.[7,30–33] Frequently, Ru nanosystems are obtained by reduction of $RuCl_3$ in glycols, such as ethylene glycol or diethylene glycol,[12,34–36] hydrogen reduction[37] or sodium borohydride reduction.[38] Ru nanoparticles are also prepared by using polymers,[39] ligands like amines, alcohols or thiols,[24,25] cellulose derivatives[40] and organosilane fragments[41] as stabilizers. However, the protected Ru nanoparticles are not stable under treatment at higher temperatures since such treatment leads to sintering of particles.[41,42]

A survey of the literature shows that most of the contributions dealing with the preparation of Ru fine nanoparticles report inconveniences such as difficult removal of solvents, high boiling point and low viscosity of the polyols

[a] Laboratory of Catalysis and Surface Chemistry, Institute of Physical Chemistry "Ilie Murgulescu", Academia Romana, 202 Splaiul Independentei, 060021 Bucharest, Romania
E-mail: josecalderonmoreno@yahoo.com
[b] Electrochemical Energy Storage Department, Chemical Sciences and Engineering Division, Argonne National Laboratory,
Argonne, Illinois 60439, USA
[c] Laboratory of Oxide Materials Science, Institute of Physical Chemistry "Ilie Murgulescu", Romanian Academy, 202 Splaiul Independentei, 060021 Bucharest, Romania

used as solvents, ligands or templating agents, also difficulties in their recyclability or the limited resistance of the nanoparticles towards sintering at high temperatures.

The objective of this paper is to report an easy, straightforward and practical thermal decomposition method that provides nanoparticles of metallic Ru protected against sintering and agglomeration up to high temperatures, without using any solvents or stabilizers, from a common available Ru compound. In comparison with the previously reported methods for preparation of carbon-supported Ru catalysts, this method is much simpler; prepared in a single step from a single commercial precursor and the pure metallic state of ruthenium nanoparticles has been confirmed by direct X-ray diffraction (XRD) and elemental analysis by electron dispersive X-ray spectroscopy (EDS). Furthermore, the fine size and dispersion of the Ru nanocrystallite is confirmed from high resolution electron microscopy and elemental mapping of Ru and C. The hydrogenation of benzene to cyclohexane has been carried out to test the catalytic activity of this carbon-supported Ru catalyst. Catalytic tests show high activity, full conversion of benzene and 100% selectivity for cyclohexane.

Results and Discussion

XRD and Raman Spectroscopy Results of Ru Particles

The XRD and Raman spectroscopy results of Ru particles are shown in Figure 1A and B, respectively. The XRD results (Figure 1A) demonstrate that the obtained particles are nanocrystalline and metallic. All the X-ray diffraction peaks are congruent with the standard ruthenium metal particles' data file (JCPDS No. 06-0663). The X-ray diffraction lines are broadened, indicating the small size of the products. The results confirm that ruthenium is one of a few transition metals that only crystallize in a hexagonal compact structure. A similar XRD pattern was measured by Bonet et al.[7] for Ru nanoparticles by microwave irradiation and an oil-bath heating method. The XRD diffraction pattern of the particles showed that no other impurity was detected in the XRD pattern.

More accurate information on the sample can be obtained from Raman spectroscopy, which is widely used for the analysis of carbon materials because of its ability to distinguish bonding types and domain size. Figure 1B shows the typical Raman spectra of the Ru/C composite particles. Bands at 1300 cm^{-1} and at 1600 cm^{-1} can be identified in the spectrum as the so-called Raman D and G bands, respectively. In Raman spectra, the G and D peaks are two typical characteristics of carbon-based materials and are identified by the E_{2g} C–C vibrational mode of the bond stretching of all pairs of sp^2 atoms and the breathing modes of the sp^2 ring structure in disordered graphite,[43] respectively. The positions and relative intensities of the D and G bands indicate a highly disordered amorphous structure, most probably because of the relatively low temperature used in the thermal decomposition. Much higher temperatures are required to initiate graphitization of the amorphous carbon. The shoulder bands at about 1250–1300 cm^{-1} (marked by *) are from the plasma lines of the laser used for the Raman measurements.

Microstructure Analysis by SEM, STEM, TEM and HRTEM

SEM micrographs of the as-prepared product are shown in Figure 2. Spherical agglomerates of 1–2 microns in size containing individual smaller particles are observed. The mean diameters of the larger round particles are estimated from the SEM images to have an average size of 1.5 microns (Figure 2A, B, C). The formation of microsized carbon spheres[44,45] and filaments[46] from organic precursors heated under autogenic pressure is well known. Fine individual particles, a few nm in size, can clearly be spotted on the surface of the microsized particles (Figure 2D).

For the EDS spectra, the Ru elemental mapping of the as-prepared product is shown in Figure 3. The typical survey spectrum shows only peaks that are characteristic of C and Ru. The absence of an O peak in the EDS measurement clearly confirms the metallic character of the Ru in the material. The homogeneous spatial distribution of Ru in the

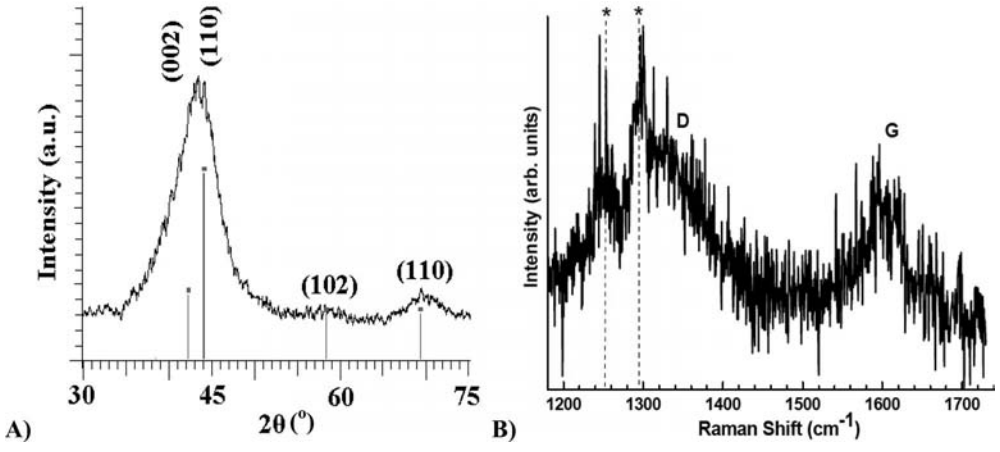

Figure 1. (A) XRD pattern of the sample, (B) Raman spectrum of the as-obtained particles.

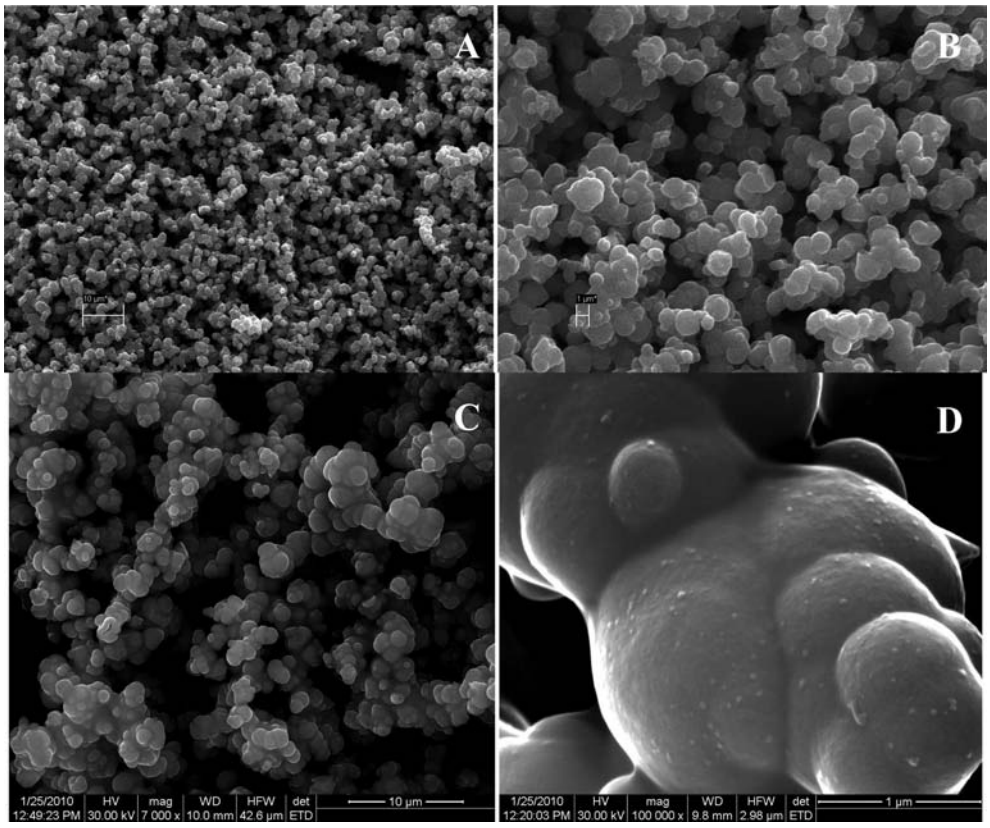

Figure 2. (A)–(D) Scanning electron micrographs of Ru/C nanocomposite.

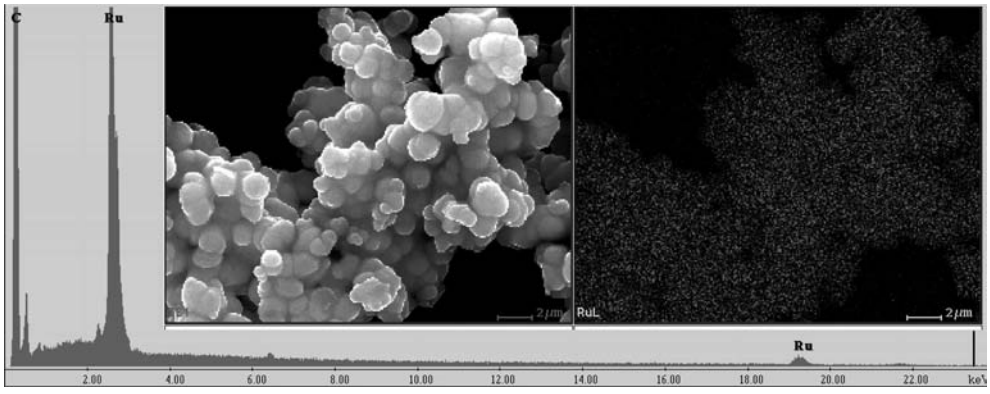

Figure 3. EDS spectrum, SEM micrograph and Ru distribution.

carbon matrix is remarkable and demonstrates the absence of Ru nanoparticle growth, sintering or agglomeration. SEM and associated EDS elemental mapping demonstrate that the product has a muffin-like structure, composed of carbon and nanosized metallic Ru well dispersed in the carbon matrix. The very fine metallic Ru clusters are embedded in the carbon matrix without any signs of agglomeration.

STEM and energy-filtered TEM confirmed the uniform distribution and small size of the Ru nanocrystallites. Figure 4 shows scanning transmission electron spectroscopy observations carried out to evidence the elemental distribution of Ru and C: the micrographs of the Ru/C nanocomposite in bright field (Figure 4A) and dark field (Figure 4B), respectively, and the elemental dot mapping of Ru (Figure 4C) and carbon (Figure 4D) in the Ru/C nanocomposite. It is well known that the thermal and chemical stability of nanosized metal particles is extremely reduced compared to the bulk system.[47] The heating of the sample to 500 °C did not cause any agglomeration in our samples or excessive particle growth of the Ru nanoparticles dispersed in the carbon matrix with a narrow size distribution. The larger Ru nanoparticles in the carbon matrix are ca. 20 nm in diameter; they are seen in Figures 2D and 4 as the darker spots in the bright-field micrograph (Figure 4A) and as the brighter spots in the dark-field image (Figure 4B).

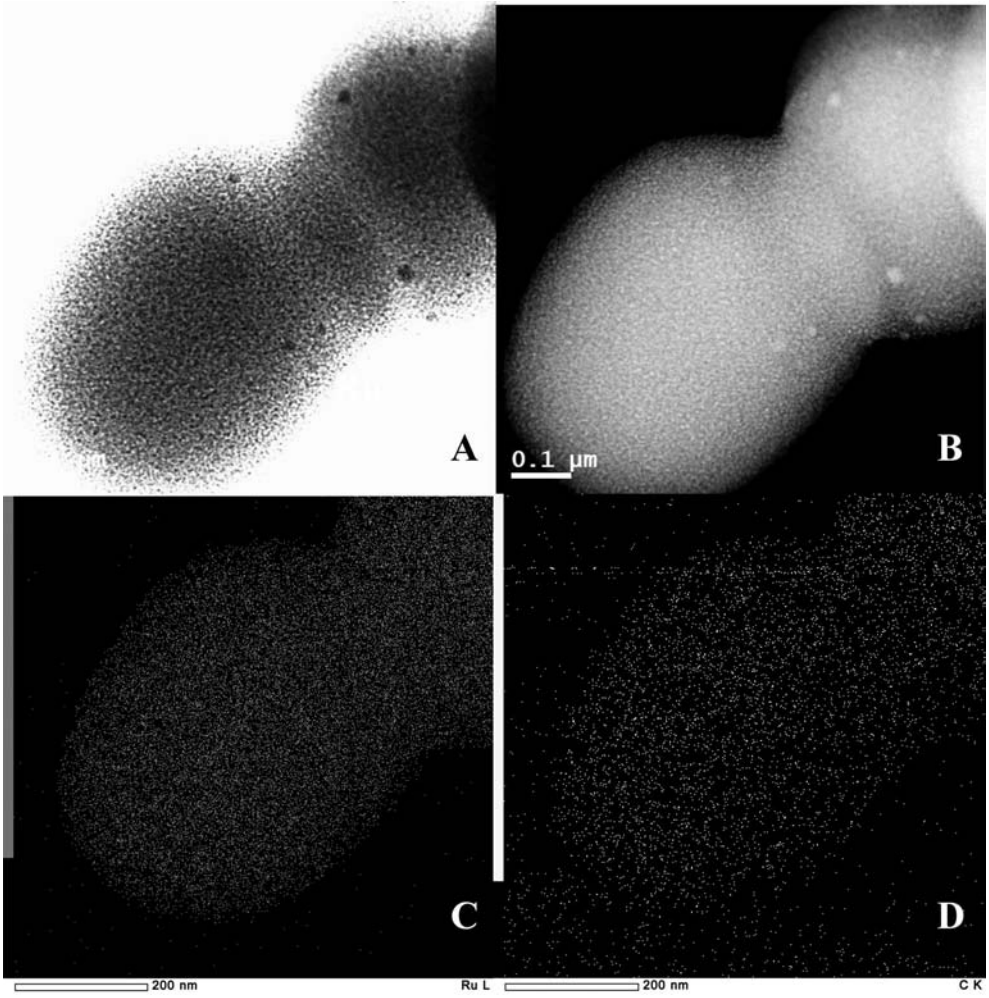

Figure 4. Scanning transmission electron spectroscopy: (A) Bright-field, (B) dark-field micrographs of Ru/C nanocomposite and elemental dot mapping of (C) Ru and (D) C.

Carbon effectively stabilizes the metallic nanoparticles rendering them air-stable, as has been reported before for Fe–Co air-stable nanoparticles.[48]

Table 1 summarizes the quantitative elemental analysis results of Ru and C as weight and mass percentages.

Table 1. Weight and atomic percent content of the Ru/C nanocomposites.

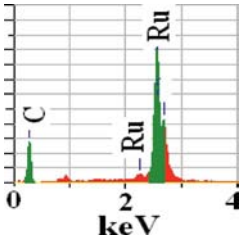

Element	[keV]	Mass [%]	Counts	Error [%]	Atom [%]
C	0.277	24.34	4447.14	0.01	73.02
Ru	2.558	75.66	15166.08	0.02	26.98

The distribution and size of metallic Ru embedded in the carbon matrix were studied at a higher resolution by TEM and HRTEM. Figure 5 shows the typical TEM images of the samples. The images clearly show dark spherical spots (Ru nanoparticles) with diameters below 5 nm (Figure 5B), well dispersed in the carbon matrix (lighter features). The higher magnification images (Figure 5C–D) reveal Ru nanocrystallites in the range 2–4 nm.

Catalytic Activity

Hydrogenation of benzene to selectively give cyclohexane by using catalysts at pressures of 20–30 atm and temperatures above 200 °C is an industrially important process in the production of nylon. The problems faced in the conventional process of benzene hydrogenation require the development of a new, effective catalyst giving the required high selectivity and conversion under milder conditions. The catalytic activity tests of the Ru/C composites for the benzene hydrogenation reaction indicate 100% conversion into cyclohexane after 2 h. The observed activity for the hydro-

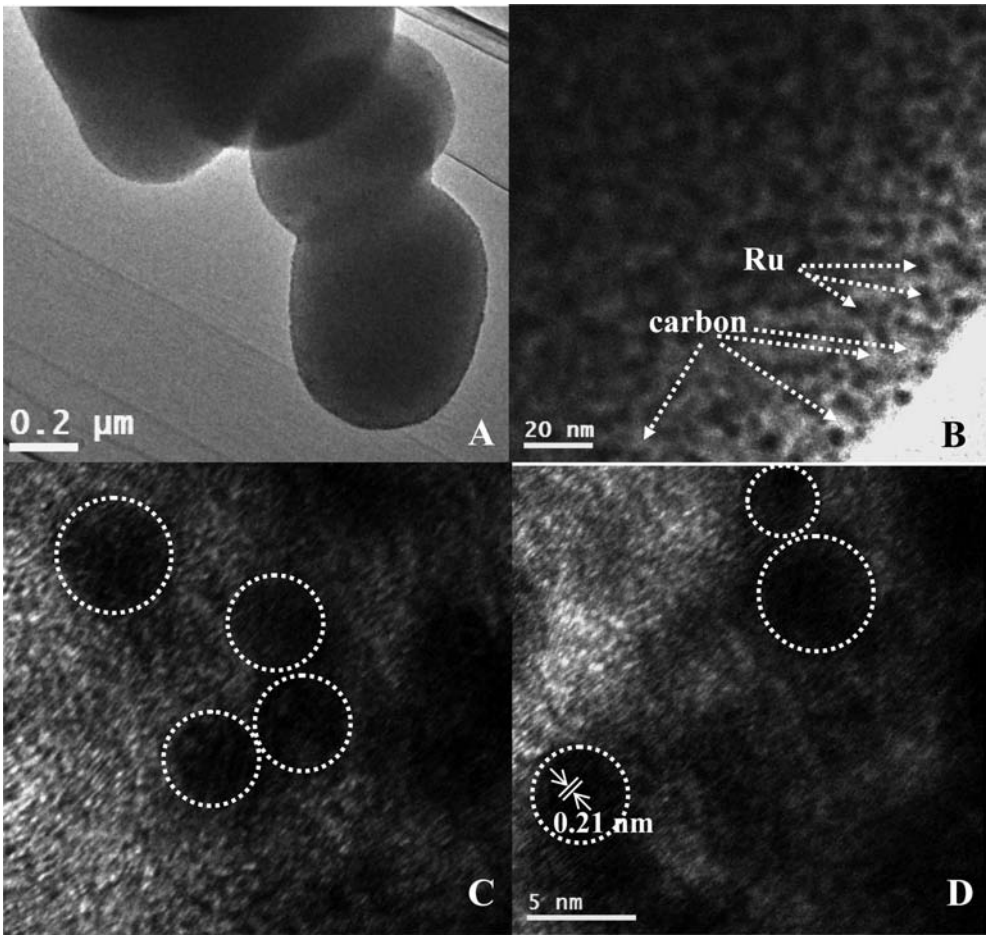

Figure 5. (A)–(D): Transmission electron micrographs of the Ru/C nanocomposite at different magnifications; (B): arrows indicate the Ru nanoparticles and carbon support. (C), (D): circles indicate the metallic Ru nanoparticles embedded in the carbon matrix.

genation of benzene to cyclohexane is much higher than the activity reported for catalytic nanoparticles supported on montmorillonite clay, a few mol per mol and hour,[49] and compares well with TOF values reported for similar catalytic test conditions for SBA and multiwall carbon nanotube supported Ru catalysts,[50,51] in the hundreds of mol per mol and hour. The recovered catalyst was reused without any change in catalytic activity.

Conclusions

We report the facile synthesis of Ru metallic nanoparticles protected in a carbon matrix in a single-step, clean, thermal decomposition, starting from a common available single precursor, Ru^{III} acetylacetonate, at a low temperature of 500 °C, without using any stabilizers or solvents. The main advantages of the process described are the versatility, efficiency, reproducibility and ease of obtaining air-stable, monocrystalline Ru particles that are a few nanometers in size and can find applications as catalysts.

Detailed microstructural observations and quantitative elemental analysis demonstrated spherical superstructures with a dense loading of Ru metal nanoparticles (75 wt.-%). The nanoparticles are homogeneous and below 5 nm in size and are uniformly embedded in a carbon matrix, forming structures like muffin cookies. The fine Ru nanoparticles are air-stable and protected against agglomeration, growth and/or sintering by the carbon-protective matrix. The as-prepared Ru/C product shows high catalytic activity for the hydrogenation reaction of benzene to cyclohexane with full conversion and selectivity at room temperature. The carbon-supported Ru nanoparticles may find further applications in other catalytic reactions at low and elevated temperatures, without microstructural changes from nanoparticle sintering or agglomeration.

Experimental Section

Synthesis: The synthesis procedure for the Ru particles is outlined in Figure 6. Ruthenium(III) acetylacetonate [$Ru(C_5H_7O_2)_3$] was purchased from Aldrich and used as received. Ruthenium(III) acetylacetonate (0.5 g) was placed in a reactor made up of Haynes 230 alloy at room temperature under atmospheric conditions. The reactor was closed and then placed at the centre of the furnace. The temperature was raised at a heating rate of 20 °C per minute up to a temperature of 500 °C, which was maintained for 2 h. The reaction took place under the autogenic pressure of the single chemical precursor. The heated reactor was gradually cooled to room temperature and opened. A dry, dark, black powder with a

40 wt.-% yield was obtained. In the reaction precursor [Ru-$(C_5H_7O_2)_3$] the calculated elemental weight percentages of carbon, hydrogen, oxygen and ruthenium are 45.2, 5.2, 24.2 and 25.4 (wt.-%), respectively. The obtained yield is around 40%. It is assumed that all the Ru from the precursor solidifies and remains (25.4 wt.-%) in the product, while around 15 wt.-% carbon nucleated to surround the formed Ru nanoparticles. The rest of the carbon and oxygen reacted to produce CO_2 gas, and at the same time hydrogen gas reacted with some of the carbon yielding additional hydrocarbons (C_xH_y), which act as reducing agents preventing the oxidation of ruthenium metal. This explains our EDS results in Table 1, where some of the carbon and most of the hydrogen and oxygen elements are lost during controlled thermolysis resulting in a higher amount of Ru compared to carbon.

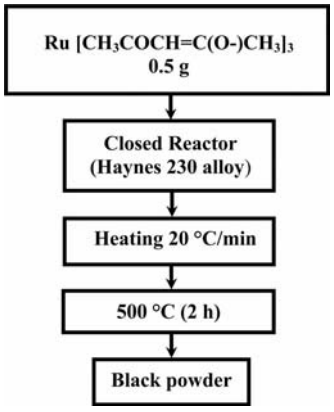

Figure 6. Synthesis procedure for obtaining the Ru nanoparticles.

Instrumental Details: Phase purity and crystal structure of the obtained Ru/C nanocomposite material were determined by using XRD. The XRD pattern was recorded with a standard diffractometer (model D5000 Siemens, Berlin, Germany) equipped with a graphite monochromator by using Cu-K_α radiation (λ = 1.5405 Å) operating at 40 mA and 40 kV and by employing a scanning rate of 0.02° and counting time of 5 s per step. Raman spectra were recorded with a Jobin–Yvon Horiba Raman system. The 514 nm line of an Ar laser was used as the excitation source, focused to a 1–2 μm spot size. The morphology of the thin films was observed by scanning electron microscopy (SEM) and transmission electron microscopy (TEM). SEM was performed by using a field-emission scanning electron microscope, JEOL JSM7500F, operating at an accelerating voltage of 10 kV. The TEM micrographs were recorded with a HITACHI HT800 apparatus equipped with a Link energy dispersive X-ray spectroscopy (EDS) system and operating at an accelerating voltage of 200 kV. The high resolution TEM and scanning transmission electron microscopy (STEM) micrographs were obtained with a JEOL 3011 microscope operating at 300 kV equipped with a high-angle annular dark-field (HAADF) detector.

Catalytic Measurement Details: Catalytic activity tests for the benzene hydrogenation reaction were performed in a stainless steel reactor. Benzene (2 mL, 0.03 mol) and the Ru/C composite catalyst (40 mg, corresponding to 3×10^{-4} mol Ru content) were loaded into the reactor. The reaction took place at a constant hydrogen pressure of 30 atm and a temperature of 25 °C under magnetic stirring. The obtained sample was analyzed by gas chromatography with a capillary column.

Acknowledgments

The paper was realized in the frame of the "Surface Chemistry and Catalysis" and "Oxide Compounds and Materials Science" Programs of the Ilie Murgulescu Institute of Physical Chemistry of the Romanian Academy, financed by the Romanian Academy.

[1] Z. F. Liu, E. T. Ada, M. Shamsuzzoha, G. B. Thompson, D. E. Nikles, *Chem. Mater.* **2006**, *18*, 4946–4951.
[2] R. Narayanan, M. A. El-Sayed, *Nano Lett.* **2004**, *4*, 1343–1348.
[3] T. S. Ahmadi, Z. L. Wang, T. C. Green, A. Henglein, M. A. El-Sayed, *Science* **1996**, *272*, 1924–1926.
[4] S. Park, S. A. Wasileski, M. J. Weaver, *J. Phys. Chem. B* **2001**, *105*, 9719–9725.
[5] S. Mukerjee, J. Mcbreen, *J. Electroanal. Chem.* **1998**, *448*, 163–171.
[6] W. P. Halperin, *Rev. Mod. Phys.* **1986**, *58*, 533–606.
[7] F. Bonet, V. Delmas, S. Grugeon, R. Herrera Urbina, P.-Y. Silvert, K. Tekaia-Elhsissen, *Nanostruct. Mater.* **1999**, *11*, 1277–1284.
[8] J. S. Bradley in *Clusters and Colloids* (Ed.: G. Schmid), VCH, Weinheim, **1994**, chapter 6.
[9] A. M. Raspolli Galletti, C. Antonetti, S. Giaiacopi, O. Piccolo, A. M. Venezia, *Top. Catal.* **2009**, *52*, 1065–1069.
[10] J. A. Dahl, B. L. S. Maddux, J. E. Hutchison, *Chem. Rev.* **2007**, *107*, 2228–2269.
[11] R. Harpeness, Z. Peng, X. Liu, V. G. Pol, Y. Koltypin, A. Gedanken, *J. Colloid Interface Sci.* **2005**, *287*, 678–684.
[12] A. Miyazaki, I. Balint, K. Aika, Y. Nakano, *J. Catal.* **2001**, *204*, 364–371.
[13] S. Chen, R. Ingram, M. Hostetler, J. Pietron, R. Murray, T. Schaaff, J. Khoury, M. Alvarez, R. Whetten, *Science* **1998**, *280*, 2098–2101.
[14] G. A. Somorjai, F. Tao, J. Y. Park, *Top. Catal.* **2008**, *47*, 1–14.
[15] J. Y. Park, C. Aliaga, J. R. Renzas, H. Lee, G. A. Somorjai, *Catal. Lett.* **2009**, *129*, 1–6.
[16] R. Narayanan, M. A. El-Sayed, *Top. Catal.* **2008**, *47*, 15–21.
[17] A. Gniewek, J. J. Ziółkowski, A. M. Trzeciak, M. Zawadzki, H. Grabowska, J. Wrzyszcz, *J. Catal.* **2008**, *254*, 121–130.
[18] Z. S. Pillai, P. V. Kamat, *J. Phys. Chem. B* **2004**, *108*, 945–951.
[19] I. M. Yakutik, G. P. Shevchenko, *Surf. Sci.* **2004**, *566–568*, 414–418.
[20] M. Liu, B. He, H. Liu, X. Yan, *J. Colloid Interface Sci.* **2003**, *263*, 461–466.
[21] W. Tu, H. Liu, *J. Mater. Chem.* **2000**, *10*, 2207–2211.
[22] M. T. Reetz, G. Lohmer, US Pat. 6,224,739, **2001**.
[23] C. Pan, K. Pelzer, K. Philippot, B. Chaudret, F. Dassenoy, P. Lecante, M. J. Casanove, *J. Am. Chem. Soc.* **2001**, *123*, 7584–7593.
[24] K. Pelzer, O. Vidoni, K. Philippot, B. Chandret, V. Colliere, *Adv. Funct. Mater.* **2003**, *13*, 118–126.
[25] A. Gedanken, *Ultrason. Sonochem.* **2004**, *11*, 47–55.
[26] Y. He, K. Vinodgopal, M. Ashokkumar, F. Grieser, *Res. Chem. Intermed.* **2006**, *32*, 709–715.
[27] H. Li, R. Wang, Q. Hong, L. Chen, Z. Zhong, Y. Koltypin, J. Calderon-Moreno, A. Gedanken, *Langmuir* **2004**, *20*, 8352–8356.
[28] K. Torigoe, K. Esumi, *Langmuir* **1993**, *9*, 1664–1667.
[29] A. B. Smetana, K. J. Klabunde, C. M. Sorensen, *J. Colloid Interface Sci.* **2005**, *284*, 521–526.
[30] F. Fievet, J. P. Lagier, B. Beaudoin, M. Figlarz, *Solid State Ionics* **1989**, *32/33*, 198–205.
[31] L. K. Kurihara, G. M. Chow, P. E. Schoen, *Nanostruct. Mater.* **1995**, *5*, 607–613.
[32] A. Miyazaki, K. Takeshita, K. Aika, Y. Nakano, *Chem. Lett.* **1998**, *4*, 361–362.
[33] G. Viau, R. Brayner, L. Poul, N. Chakroune, E. Lacaze, F. Fievet Vincent, F. Fievet, *Chem. Mater.* **2003**, *15*, 486–494.
[34] I. Balint, A. Miyazaki, K. Aika, *J. Catal.* **2003**, *220*, 74–83.

[35] J. Okal, M. Zawadzki, L. Kepinski, L. Krajczyk, *Appl. Catal. A* **2007**, *319*, 202–209.
[36] J. Okal, L. Kepinski, *Catal. Lett.* **2009**, *128*, 331–336.
[37] G. Lafaye, Ch. T. Williams, M. D. Amiridis, *Catal. Lett.* **2004**, *96*, 43–47.
[38] M. Liu, W. Yu, H. Liu, J. Zheng, *J. Colloid Interface Sci.* **1999**, *214*, 231.
[39] Y. Chen, K. Y. Liew, J. Li, *Mater. Lett.* **2008**, *62*, 1018–1021.
[40] A. Duteil, R. Queau, B. Chaudret, R. Mazel, C. Roucau, J. S. Bradley, *Chem. Mater.* **1993**, *5*, 341–347.
[41] K. Pelzer, J. P. Candy, G. Bergeret, J. M. Basset, *Eur. Phys. J. D* **2007**, *43*, 197–200.
[42] M. José-Yacaman, C. Gutierrez-Wing, M. Miki, D.-Q. Yang, K. N. Piyakis, E. Sacher, *J. Phys. Chem. B* **2005**, *109*, 9703–9711.
[43] J. M. C. Moreno, S. S. Swamy, T. Fujino, M. Yoshimura, *Chem. Phys. Lett.* **2000**, *329*, 317–322.
[44] V. G. Pol, S. V. Pol, J. Calderon-Moreno, A. Gedanken, *Carbon* **2006**, *44*, 3285–3292.
[45] B. Basavalingu, J. M. C. Moreno, K. Byrappa, Y. G. Gogotsi, M. Yoshimura, *Carbon* **2001**, *39*, 1763–1767.
[46] V. G. Pol, S. V. Pol, B. Markovsky, J. Calderon-Moreno, A. Gedanken, *Chem. Mater.* **2006**, *18*, 1512–1519.
[47] Q. L. Li, H. L. Li, V. G. Pol, I. Bruckental, Y. Koltypin, J. Calderon-Moreno, I. Nowik, A. Gedanken, *New J. Chem.* **2003**, *27*, 1194–1199.
[48] V. G. Pol, S. V. Pol, J. Calderon-Moreno, A. Gedanken, *Carbon* **2006**, *44*, 3285–3292.
[49] J. Huang, T. Jiang, B. X. Han, W. Z. Wu, Z. M. Liu, Z. L. Xie, J. L. Zhang, *Catal. Lett.* **2005**, *103*, 59–62.
[50] Z. Y. Sun, Z. M. Liu, B. X. Han, J. M. Du, Z. L. Xie, G. J. Han, *Adv. Mater.* **2005**, *17*, 928–932.
[51] S. B. Halligudi, H. C. Bajaj, K. N. Bhatt, M. Krishnaratnam, *React. Kinet. Catal. Lett.* **1992**, *48*, 547–552.

Received: December 29, 2010
Published Online: May 17, 2011

